NAVAL POSTGRADUATE SCHOOL
Monterey, California

THESIS

REDUCING THE SUSCEPTIBILITY OF
LOW SPEED / LOW MANOEUVRABILITY
AIRCRAFT TO
INFRARED MISSILE KILLS

by

Chia, Hock Teck

Dec 1989

Thesis Advisor — Prof. Alfred W. Cooper
Co-Advisor — Prof. Robert E. Ball

REPORT DOCUMENTATION PAGE

1a Report Security Classification: Unclassified		1b Restrictive Markings	
2a Security Classification Authority		3 Distribution Availability of Report: Approved for public release; distribution is unlimited.	
2b Declassification Downgrading Schedule			
4 Performing Organization Report Number(s)		5 Monitoring Organization Report Number(s)	
6a Name of Performing Organization: Naval Postgraduate School	6b Office Symbol (*if applicable*): 3A	7a Name of Monitoring Organization: Naval Postgraduate School	
6c Address (*city, state, and ZIP code*): Monterey, CA 93943-5000		7b Address (*city, state, and ZIP code*): Monterey, CA 93943-5000	
8a Name of Funding Sponsoring Organization	8b Office Symbol (*if applicable*)	9 Procurement Instrument Identification Number	
8c Address (*city, state, and ZIP code*)		10 Source of Funding Numbers	
		Program Element No	Project No / Task No / Work Unit Accession No

11 Title (*include security classification*): REDUCING THE SUSCEPTIBILITY OF LOW SPEED / LOW MANOEUVRABILITY AIRCRAFT TO INFRARED MISSILE KILLS

12 Personal Author(s): Chia, Hock Teck

13a Type of Report	13b Time Covered	14 Date of Report (*year, month, day*)	15 Page Count
Master's Thesis	From To	Dec 1989	55

16 Supplementary Notation: The views expressed in this thesis are those of the author and do not reflect the official policy or position of the Department of Defense or the U.S. Government.

17 Cosati Codes			18 Subject Terms (*continue on reverse if necessary and identify by block number*)
Field	Group	Subgroup	Infrared countermeasures, aircraft survivability.

19 Abstract (*continue on reverse if necessary and identify by block number*): Low speed / low manoeuvrability aircraft are currently quite susceptible to being killed in attacks by the ubiquitous infrared missiles. A theoretical analysis applied to an encounter simulation seems to indicate that it is possible to use the infrared jammer to defeat second generation infrared missiles. The theoretical analysis of a simplified case of a conical scan reticle with frequency modulation jamming leads to expressions for the target's position, as seen by the missile seeker, under no-jamming and under infinitely-powerful-jamming conditions. The intermediate-power case is dealt with by numerical analysis for a selected, non-optimal situation, as the closed form solution is not immediately apparent. The analysis indicates successful jamming in the situation studied. In the scenario where the infrared missile is an almost continuous threat during the aircraft's flight, infrared jammers and low visual signature paints, and perhaps low infrared signature paints, are short-term solutions that are potentially useful in increasing the survivability of these aircraft by reducing their susceptibility to infrared missile kills.

20 Distribution Availability of Abstract	21 Abstract Security Classification	
☒ unclassified unlimited ☐ same as report ☐ DTIC users	Unclassified	
22a Name of Responsible Individual: Prof. Alfred W. Cooper	22b Telephone (*include Area code*): (408) 646-2452	22c Office Symbol: 61Cr

DD FORM 1473,84 MAR — 83 APR edition may be used until exhausted / All other editions are obsolete

Approved for public release; distribution is unlimited.

Reducing the Susceptibility of Low Speed / Low Manoeuvrability Aircraft to Infrared Missile Kills

by

Chia, Hock Teck
Major, Republic of Singapore Air Force
B.Eng., University of Singapore, 1980

Submitted in partial fulfillment of the
requirements for the degree of

MASTER OF SCIENCE (SYSTEMS ENGINEERING)

from the

NAVAL POSTGRADUATE SCHOOL
Dec 1989

ABSTRACT

Low speed / low manoeuvrability aircraft are currently quite susceptible to being killed in attacks by the ubiquitous infrared missiles. A theoretical analysis applied to an encounter simulation seems to indicate that it is possible to use the infrared jammer to defeat second generation infrared missiles. The theoretical analysis of a simplified case of a conical scan reticle with frequency modulation jamming leads to expressions for the target's position, as seen by the missile seeker, under no-jamming and under infinitely-powerful-jamming conditions. The intermediate-power case is dealt with by numerical analysis for a selected, non-optimal situation, as the closed form solution is not immediately apparent. The analysis indicates successful jamming in the situation studied. In the scenario where the infrared missile is an almost continuous threat during the aircraft's flight, infrared jammers and low visual signature paints, and perhaps low infrared signature paints, are short-term solutions that are potentially useful in increasing the survivability of these aircraft by reducing their susceptibility to infrared missile kills.

DISCLAIMER

The reader is cautioned that computer programs developed in this research may not have been exercised for all cases of interest. While every effort has been made, within the time available, to ensure that the programs are free of computational and logic errors, they cannot be considered validated. Any application of these programs without additional verification is at the risk of the user.

TABLE OF CONTENTS

LIST OF TABLES

LIST OF FIGURES

ACKNOWLEDGEMENTS

The assistance of Prof. Daniel J. Collins, in obtaining the TACTICS IV program and in providing information on missile guidance, is gratefully acknowledged.

I. INTRODUCTION

A. BACKGROUND

When low speed / low manoeuvrability aircraft operate from bases which cannot be secured to a sufficiently great depth (more than several kilometres), they are vulnerable to surface-to-air missiles (SAM). As small, man-portable SAMs are quite readily available, they constitute a high probability threat.

When out of the SAM engagement envelope, air-to-air missiles (AAM) remain as potential threats to these aircraft.

B. SCOPE

This thesis will address a particular aspect of this threat - the threat by infrared (IR) guided missiles. This is because infrared missiles are ubiquitous and rather successful, as can be seen in Table 1 on page 2 ((General Dynamics,1988), (Loral,1989) and (Nicholas,1988)) and Table 2 on page 3 (Loral,1988,Slide 87329).[1]

For this thesis, we will consider aircraft that are already deployed (as opposed to an aircraft still to be designed). Therefore the scope of survivability enhancement by vulnerability reduction is more limited than increasing survivability by susceptibility reduction.[2]

Hence we will concentrate on the (hopefully) easier task of finding measures to reduce the susceptibility of these aircraft to being hit by an infrared missile.

Due to U.S. Government restrictions on dissemination of security-sensitive information, this thesis is required to be unclassified. This constrains the thesis to a more generic treatment of the problem.

C. GENERAL SCENARIO

For the purposes of this thesis, the scenario is that the aircraft launches from a base that can only be secured to a depth of a few kilometers. i.e.,the aircraft is within the acquisition and launch envelope of threat missiles (especially easily-concealed man-portable SAMs) on takeoff as well as during the landing phase of flight. (An example

---

1 Quoted from Moore D.,(OSD), *23rd IRIA/IRIS 1985 IRCM Symposium,* p.1 A-2, 1985.

2 The terms used here are from Ball (1985). The probability of kill of an aircraft (P_k) is the product of probability of hit by a threat weapon (P_h) and the probability of kill given that the aircraft is hit ($P_{k/h}$). Susceptibility is associated with the probability of hit whereas vulnerability is probability of kill given a hit by the threat weapon.

Table 1. QUANTITIES OF MISSILES

: (Shows the extent of the threat.)

Name	Designation	Origin	Type	Deployed	Quantity
Acrid	AA-6	USSR	AAM	?	?
Alamo	AA-10	USSR	AAM	?	?
Anab	AA-3	USSR	AAM	1972	O(3)
Apex	AA-7	USSR	AAM	1975	?
Aphid	AA-8	USSR	AAM	1976 (?)	?
Archer	AA-11	USSR	AAM	?	?
Ash	AA-5	USSR	AAM	1961	O(3)
Atoll	AA-2	USSR	AAM	Early 1960s	?
Chaparral	MIM-72	USA	SAM	1979	10 000+
Firestreak	-	UK	AAM	?	?
Gaskin	SA-9	USSR	SAM	1968	?
Gopher	SA-13	USSR	SAM	1981	200
Grail	SA-7, SA-N-5	USSR	SAM	1972	50 000+
Gremlin	SA-14	USSR	SAM	?	?
HN-5A C	HN-5A C	China	SAM	1988	?
Keiko	Type 81	Japan	SAM	?	?
Kukri	V3B	S. Africa	AAM	?	?
Magic	R.550	France	AAM	1985	10 000
Mica	-	France	AAM	?	?
Mistral	-	France	AAM	?	?
Piranha (?)	MAA-1	Brazil	AAM	1989	?
Python	-	Israel	AAM	?	?
RB-72	RB-72	Sweden	AAM	?	?
Redeye	FIM-43	USA	SAM	1966	?
Redtop	?	UK	AAM	?	?
Shafrir	?	Israel	AAM	?	?
Sidewinder	AIM-9L,M	USA	AAM	1977,1982	150 000
Stinger	FIM-92A	USA	SAM	1979	15 000+
Stinger-POST	?	USA	SAM	1982	53 000

Note: O(n) means of the order of magnitude of 10^n.

Table 2. KILLS OF AIRCRAFT BY WEAPON TYPE
: (Note the large fraction of infrared missiles.)

Type	Kills	Fraction
Infrared missiles	135+ to 146+	93%
Radar missiles	2	1%
Gunfire	8+ to 10+	6%

of this aspect of the scenario is an Antonov An-26 or Antonov An-32 aircraft operating out of Kabul.) The aircraft then climbs to its cruising / operating altitude, typically between 5 and 30 thousand feet. While it is at medium altitude, the more likely infrared missile threat is that of the AAM.

Additionally, it is assumed that the launch platform of the infrared missile can reach a position such that the aircraft is within the acquisition and or launch envelope of the missile. The aircraft, which is usually unarmed, is unassisted by other aircraft and lacks the speed to run away from an airborne threat.

Since infrared missiles are fire-and-forget weapons, multiple infrared missiles can attack the same target. Therefore, this threat must also be handled. However, we will also assume that the multiple infrared missiles are of one type, during one attack.

II. THE AIRCRAFT CHARACTERISTICS

A characterization of the aircraft in terms of the factors significant to the infrared missile countermeasure problem are as follows:-

A. GENERAL INFRARED SIGNATURE FACTORS

The infrared signature of an aircraft is dependent, to various degrees, on a number of factors. Various energy sources (and sinks) cause heating (and cooling) of the aircraft, and also reflect off aircraft surfaces. The energy is distributed over the aircraft primarily by conduction and radiation (and convection, in the case of the engine exhaust plume). The surface temperature and the surface spectral emissivity together determine the emitted power. The incident energy, geometry and spectral reflectance determine the reflected energy component of the infrared signature. A summary list of the various components follows (Higby,1972). (Where available, typical values are also quoted (Loral,1988,Slide 91537).)

1. Emission component energy sources/sinks

- Engine (thermodynamic cycle)
  (Hot metal typically emits 1 kW/sr/μm at > 1.5 μm)
  (Engine exhaust shroud typically emits 100 W/sr/μm > 3 μm)
- Engine exhaust plume (Typically emits 50 W/sr/μm at 3.8 μm to 4.8 μm)
- Avionics/Heat pumps.
- Solar heating
- Aerodynamic heating via adiabatic effects and friction/viscous effects. Aerodynamic heating is not significant at the speed at which these aircraft fly. (< 400kts IAS).
- Radiation exchange with atmosphere and via nocturnal cooling.
- Free stream conduction (Skin surface emission is typically 10 W/sr/μm at 8 μm to 14 μm)

2. Surface emissivity

Total emissivity (as opposed to spectral emissivity) is around 0.9 for the more normal painted surfaces.

3. Reflection component energy sources

In addition to the emission component energy sources (which are also reflection component energy sources), the other energy sources include:-

- Sun - Sunlight reflecting off aircraft surfaces, particularly when specular reflection occurs, is known as glint. At typical values of 100 W/sr/μm at < 3 μm, sunlight reflection is a significant contributor to the infrared signature, when it is present.
- Sky - This is indirect sunlight, scattered by the atmospheric components (e.g., clouds).
- Ground (earthshine) - Again this is indirect sunlight, i.e., sunlight reflected off the earth's surface or infrared radiation coming from the heated earth's surface.

4. Reflectance

These values are highly variable in the infrared bands for painted surfaces, such as these aircraft would have.

5. Geometry/Structure

While not directly a source of energy, the geometry of the aircraft does determine how the infrared energy is spatially distributed. Geometrical effects include:-

- Multiple reflections - The "energy packets" reflect off several surfaces before they reach the infrared detector. This redirects the infrared energy in complex ways.
- Absorption/re-emission sites - Where a site is in relation to the energy source will determine whether it will absorb energy by radiation and/or convection.
- Shielding - The energy source is masked by aircraft structures between the source and the infrared detector.
- Shadowing - Part of a surface that appears darker because the energy source is shielded from that surface by intervening aircraft structures.
- Engine exhaust plume shape and size - This is a function of the engine operating conditions and the airflow field around the aircraft.
- Aerodynamic heating - This arises from adiabatic compresssion of air and from drag. Where this occurs, and the degree to which it occurs, is again determined by the shape, size and position of the aircraft structures.

6. Atmospheric transmission

The atmosphere is a selective absorber. (Cooper,1988.p.1-6) In the infrared bands, there are two windows, one at 3 μm to 5 μm and the other at 8 μm to 14 μm waveband. Most of the detectors used in infrared missiles seekers are designed to work in these windows. Most detectors are still using the 3 μm to 5 μm waveband window.

B. INFRARED SIGNATURE VS. PHASES OF FLIGHT/MISSION

The takeoff and climbout infrared signatures of an aircraft are significantly greater than during the cruise, on-station, descent or landing phases. The exhaust gas temperature varies by a factor of 2 or more between these phases of flight.

C. INFRARED SIGNATURE MODELS AND MEASUREMENTS

Many infrared signature models exist. However, the more readily available ones only model the engine and only the jet-engine. e.g.,PIREPS (GEC, 1976) and ASDIR (ASD-WPAFB, 1975). There was no trace in the open literature of infrared models dealing with the turboprop engine, which typically power these aircraft. A few, (e.g, HIDE (Higby, 1972)) do consider the other factors such as skin surface emissions. Neither infrared signature models nor measured signatures of aircraft were available for inclusion in this thesis. It should be noted that there is a lot of similarity of these models to the surface rendering models found in CAD/CAM applications.

The true infrared signature of the particular aircraft, which we desire to protect, needs to be verified and/or determined by actual measurement with appropriate radiometers. (In the analysis that follows, only the relative radiant intensity of the jammer with respect to the aircraft is required. However, the absolute power of the jammer can only be specified if the aircraft infrared signature values are known.)

D. VULNERABILITY

Since vulnerability of an aircraft is defined as the probability of kill, given a hit, the definition of "kill" strongly influences the value of P_k . Aircraft kill would be when the aircraft is destroyed. However, if a kill is defined as denial of mission, then the P_k may be larger, since electronic equipment, other support equipment and human operators are all susceptible to serious mission-hindering damage.

E. MANOEUVRABILITY

Low speed / low manoeuvrability aircraft are quite far, in flight performance, from an agile fighter aircraft. The climb rate of the low speed / low manoeuvrability aircraft is typically of the order of a few thousand feet a minute and their speed is in the low hundreds of knots. Acceleration normal to the aircraft's forward flight is limited to a few times gravity. This prohibits evasion of contact by acceleration and jinking.

III. THREATS AND THE ENVIRONMENT

A. INFRARED MISSILE SYSTEM

Here are some typical features of infrared missiles.

1. Airframe and propulsion

Usually the infrared missile has a cylindrical body with cruciform delta and/or trapezoidal wings and canards. The nose is blunt and transparent at the infrared waveband of interest. Propulsion for AAMs tends to be from single stage motors. SAMs, on the other hand, are often two-staged motors, with a booster to get the missile up to flying speed rapidly and then a sustainer motor for continuing the flight. The flight performance is characterized by the acceleration and velocity vectors attainable as a function of time, and the maximum ranges this gives.

2. Seeker

a. Sensor

Earlier generation detectors were made with lead sulphide. Indium antimonide is more widely used nowadays. Lead sulphide detectors work around the 3 μm waveband whereas the detectivity of cooled indium antimonide peaks at around 5 μm. This allows the cooled indium antimonide detectors to work with radiation from all aspects with respect to the aircraft. This is in contrast to lead sulphide which can only work with the hot engine parts and engine plume. (Cooper,1988,pp.2-22,7-21)

To accomodate the wide range (> 70 dB) in the scene and target irradiance as the missile flies towards its target, the detector is normally backed by an amplifier with Automatic Gain Control (AGC), so that the downstream processors have a normalized signal to work with. Significant parameters here are the attack and decay response times of the AGC and the saturation level.

b. Optics and stabilization

There is usually a telescope in front of the detector to gather the infrared energy. To maintain the seeker line-of-sight with narrow beamwidth optics, the telescope is normally decoupled from the missile body motion. i.e., the telescope is stabilized in inertial space. Significant parameters here are the maximum slew rates and the gimbal limits and the instantaneous field of view which is a function of the focal length of the optics and the size of the detector.

c. Target discrimination/position determination

The determination of the target existence and position in the presence of background scene 'noise' is accomplished by various means. Early generation missiles had rotating reticles. In this scheme, information is extracted from the envelope of the detected signals. i.e., amplitude modulation (AM). This was followed by stationary reticles with the scene moved (nutated) over the reticle. Information, in this case, is carried in the frequency modulation (FM). Both these schemes transform spatial information into time and lose spatial discrimination. More recently, pseudo-imaging sensors have been used that scan the scene with a spot (or spots). For mechanical convenience, rosette scan patterns are used. The size of the spot is usually of the order of magnitude of the target image size. In the future, even more information extraction will be possible with imaging systems that can determine target features within the whole target. The effort here is to increase the ability of the sensor to determine smaller signature targets at longer ranges in the presence of higher scene 'noise', (from both natural and intentional 'noise'.)

3. **Guidance**

The guidance law for many (perhaps most) infrared missiles nowadays is proportional navigation of some sort. The proportional navigation 'constant' may vary during the flight of the missile.

The tracking loops are used to control the missile. The details of these determine the missile response to aircraft manoeuvring and target position noise (e.g., glint). The usual tradeoff between controllability and stability applies.

4. **Steering**

Steering is accomplished by one or a combination of aerodynamic surfaces or vectored thrust. To save mechanical complexity, some missiles can only apply normal forces in one axis relative to their body coordinates, and depend on the rolling of the body to align the force in the direction desired.

5. **Fuze**

Most AAMs are both proximity fuzed and contact fuzed. The field of view of the fuze and the triggering range and velocity determine the detonation point. Radar and infrared (coherent and non-coherent) fuzes are employed.

Smaller man-portable infrared SAMs are contact fuzed. Man-portable missiles need to be light in weight. Putting in a more complex, and hence larger, fuze, would require a reduction in warhead size, for a given weight limit and missile maximum range

(amount of propellant). The smaller warhead would then be less effective in killing an aircraft at the longer range at which the fuze could trigger.

6. Warhead

Missile warheads are usually high explosive blast or high explosive blast fragmentation warheads. The pattern and the nature of the damage mechanism dictate how the aircraft will fare in a near miss.

B. MISSILE ENGAGEMENT PHASES

The engagement process goes through the phases of detection, acquisition, launch, flyout and detonation. Intervention in the engagement process is possible at any stage.

C. LAUNCH PLATFORMS

The launch platforms for SAMs range from a man to vehicles. They can be very difficult to locate. Usually AAMs are carried by fighter aircraft, though, of late, they are increasingly being carried by helicopters.

D. OPERATIONS

The method of operation of the missile, e.g., where the threat is likely to be, when, etc., are significant, but the combinations are many and they depend heavily on intelligence-derived information. This topic will not be discussed further here.

E. ENVIRONMENT

The urban environment that is given in the scenario means that the background clutter is higher than it would be in a rural environment. This makes missile engagements of targets more difficult in such environments.

IV. RESPONSE

In the scenario of this thesis, the aircraft is highly susceptible to successful attack by infrared missiles. Countermeasures have therefore to be devised that can increase the likelihood of the aircraft continuing its mission. Some possible countermeasures are now discussed.

A. LAUNCH SYSTEM DESTRUCTION

Destruction of the infrared missile launcher is difficult because man-portable infrared SAMs are easily concealed.

B. LAUNCHER ACQUISITION ENVELOPE AVOIDANCE

In the scenario given, avoidance of the acquisition envelope of the launcher is not possible due to the limited geographic depth assumed.

C. LAUNCHER ACQUISITION ENVELOPE REDUCTION

Reducing the acquisition envelope of the launcher is possible because the acquisition is often visual for infrared missile engagements. Low visual signature paint schemes are required.

D. THREAT PROPAGATOR DESTRUCTION

Destruction of the missile in flight can be achieved either directly by directed energy weapons (DEW) or by triggering the fuze of proximity fuzed missiles. The DEW approach involves first detecting the missile, tracking it, and then attacking the airframe or tracking/guidance system, or the fuzing system. DEWs (laser, electromagnetic or charged particle beam) are not yet available for operational use. Electromagnetic pulse triggering of the warhead is also a future option. Pointing of those weapons is also problematic because the missile has to be tracked first. If the spot scanning seeker proves difficult to avoid (see below) , then it may be necessary to make this a viable option. Proximity fuzes tend to be sensitive in the direction perpendicular to the longitudinal axis of the missile so that they are difficult to access for self-protection i.e., from the forward direction. While it is possible to trigger them, it may not be straightforward to put enough signal into the fuze early enough to be useful.

E. THREAT PROPAGATOR AVOIDANCE

The threat propagator can be avoided by out accelerating the missile and/or by manipulating the seeker's tracking ability. It is very unlikely that low speed / low manoeuvrability aircraft can out-manoeuvre a missile because these aircraft cannot generate a large enough acceleration vector and/or displacement from the missile's flight path. Also, this method would require a reliable means of determining the presence and location of the missile. Manipulating the seeker can be achieved by reducing the signal provided to the seeker, increasing the noise at the seeker or providing other (false) targets for the seeker.

1. Reduce signal

This can be accomplished by reducing the aircraft's infrared signature. This can be done intermittantly, e.g., by engine power reductions at critical points in time, or continuously. For the latter, hot parts can be shielded (insulated) and airflow altered to mix with and/or cool the hot parts. This will require structural and aerodynamic work to execute.

For reflected energy reduction, low infrared signature paints can be considered. A potential problem with these paints is that the thermal load on the aircraft will increase (Ball,1988,p.293).

Another technique is by 'capturing' the Automatic Gain Control (AGC) of the amplifier of the missile's detector. Essentially, this involves depositing enough energy on the detector for a brief period (of the order of the attack time of the AGC) to cause the gain of the detector amplifiers to decrease to the extent that the real target signal is lost in the noise. The period of energy deposition has to be brief, or else the real target signature is actually enhanced, which is the opposite of the intention. To keep the detector blind for a prolonged period, this energy pulse is repeated before the AGC can decay completely. The overall intent is to keep the signal available to the missile processing electronics as low as possible. The technique works particularly against missile seekers that derive information from the envelope of the signal, as the first generation AM seekers do.

2. Increase noise

Noise can be increased either by tactical use of natural sources, such as by placing the target up-sun of the missile launch platform, or by deliberate use of high-powered infrared sources. For the latter case, if the noise source does not saturate the detector, it may very well provide a much stronger signal for the missile to home on, i.e., become a beacon.

3. False signals

Flares are a commonly used means of countering infrared missiles. They are, however, expendables. In the case of these aircraft which will remain (because they generally have low excess power) for several minutes in the acquisition envelope of the infrared missile, reliable warning of the presence of the missile must be available to trigger flare release. Current false alarm rates and probability of detection of present day missile warning equipment are not adequate for this task. Because of the lack of manoeuvrability of these aircraft, separation of the flare from the aircraft, if needed, will not be aided greatly by manoeuvre. Rather, the ejection speed of the flare and gravity will be the determinant of the rate of shift of the centroid of the target and flare signatures.[3] Moreover, flares with the combination of the right spectral quality (to defeat multi-colour seekers), quick burn build up and long burn time with low weight, are not readily available. Flares may also be difficult to use on takeoff, if the takeoff path is over populated areas.

Modulation of an infrared source to provide misleading signals to the seeker can be done. (Devices used for this purpose will be called infrared jammers.) Against AM seekers, in addition to the AGC capture, the phase of the envelope variations can be manipulated by the infrared jammer and so the position vector determined by the seeker will be false. We do not deal with these seekers here as it is assumed that they are relatively easy to deal with. The second generation missile seekers tend to be conscan (FM) types. An analysis done to determine the potential of the infrared jammer to deceive such a seeker has been carried out and shows that it potentially can do so, as will be discussed later in Section "V. Conscan (FM) seeker vs. infrared jammer" of this thesis. Because of the narrow instantaneous field of view of a spot scanning seeker, it is unlikely that significant false signals can be inserted into these seekers in this way.[4]

---

3 It may, on occasion, be useful to have a low separation speed against a spot seeker missile that uses kinematic following to try to defeat flares. In that case, the missile miss distance will be small. Therefore, this can only work if the missile does not have a proximity fuze.

4 While the spot seeker missile must be dealt with, readily available information on these missiles is lacking. Therefore, with the time constraints of this study, we can only speculate on possible countermeasures against these missiles.

V. CONSCAN (FM) SEEKER VS. INFRARED JAMMER

A. BACKGROUND TO THE ANALYSIS

This is a reticle in which the image is moved (nutated) over a stationary reticle. The resulting frequency modulation of the signal out of the detector can be processed to extract the 2-D position of the target relative to the reticle centre.

The following analysis is derived from papers by Gedance(1961) and Suzuki(1979).

Gedance's analysis is for a target in the form of an illuminated disk of uniform and constant irradiance, and a spoked (or wagon wheel) reticle with a transmissivity function that is either one or zero as a function of the azimuth of the reticle. His analysis stops at the determination of the instantaneous frequency generated by the target image on the reticle. He does not derive the 2D position of the target.

Suzuki considers a point target for a reticle similar to that analysed by Gedance. Suzuki then shows the relations necessary to obtain the 2D position of the target.

Neither Gedance nor Suzuki deals with the jamming case which the following analysis does include.

B. ANALYSIS

In the following analysis, we want to determine the apparent target position, as seen by the seeker, while under jamming. To do so, we obtain, in order, the flux seen by the detector, then the instantaneous frequency of the flux signal and, finally, the expressions for the target position, as determined by the seeker. The expressions for the target position will be for the two extreme cases of no-jammer and for an infinitely-powerful-jammer. Only one case is dealt with here for the intermediate-jammer-power range. This is because the general solution to this case is not immediately apparent and hence a numerical analysis had to be used.

C. FLUX SIGNAL

Assume a uniformly illuminated target disk of radius δ moving in a circular path of radius r about the origin O_{ROT} (See Figure 1 on page 14.) The position of this origin, with respect to the reticle centre O_{RET}, is in fact the "position" of the target with respect to the seeker boresight. The target image centre is at (D, α) with respect to the reticle centre O_{RET}.

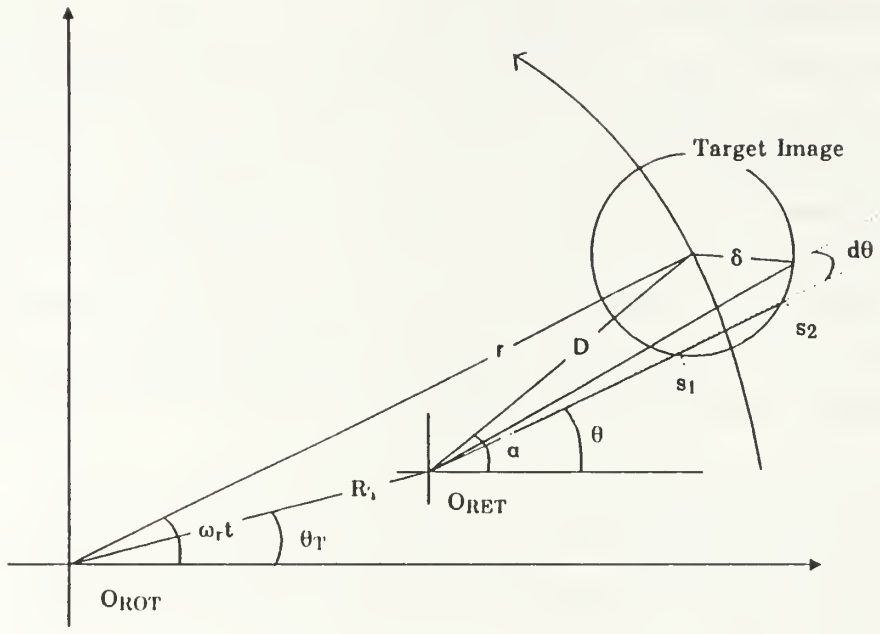

Figure 1. Reticle-Target Geometry

In general, the flux, $F(t)$, transmitted through a reticle is given by

$$F(t) = I(t)\int_A T(s, \theta)dA \tag{1}$$

where

$I(t) \triangleq$ irradiance of the image,

$A \triangleq$ area of the image,

$(s, \theta) \triangleq$ polar coordinates relative to the reticle centre O_{RET},

$T(s, \theta) \triangleq$ transmissivity of the reticle.

The equation of the circle that describes the target image is given by

$$\delta^2 = s^2 + D^2 - 2sD\cos(\alpha - \theta) \tag{2}$$

Solving for s , in the above equation, we get the two roots

$$s_1 = D\cos(\alpha - \theta) - \sqrt{D^2\cos^2(\alpha - \theta) - (D^2 - \delta^2)} \tag{3}$$

$$s_2 = D\cos(\alpha - \theta) + \sqrt{D^2\cos^2(\alpha - \theta) - (D^2 - \delta^2)} \tag{4}$$

The elemental area, dA , is approximated by a rectangle of width $\left[\left(\frac{s_2 + s_1}{2}\right)d\theta\right]$ and side lengths $(s_2 - s_1)$. Therefore, the incremental area is

$$dA = (s_2 - s_1)\left[\left(\frac{s_2 + s_1}{2}\right)d\theta\right] \tag{5}$$

From Eqns. (1), (3), (4) and (5), the flux $F(t)$ is now

$$F(t) = I(t)2D\int_{\alpha - \arcsin\left(\frac{\delta}{D}\right)}^{\alpha + \arcsin\left(\frac{\delta}{D}\right)} T(s, \theta)\cos(\alpha - \theta)\sqrt{D^2\cos^2(\alpha - \theta) - (D^2 - \delta^2)}\, d\theta \tag{6}$$

If the reticle transmittance is independent of the radius, s , i.e., the reticle is a radially symmetric reticle, then

$$T(s, \theta) = T(\theta) \tag{7}$$

And if $T(\theta)$ is a periodic pattern of period $2L\ (= \frac{2\pi}{m})$, it can be described as a Fourier Series thus:

$$\begin{aligned} T(\theta) &= \frac{c_0}{2} + \sum_{n=1}^{\infty} c_n \cos\left(\frac{n\pi\theta}{L} + \phi_n\right) \\ &= \frac{c_0}{2} + \sum_{n=1}^{\infty} c_n \cos(nm\theta + \phi_n) \end{aligned} \tag{8}$$

where

$$c_n = \frac{m}{\pi} \int_{-\frac{\pi}{m}}^{\frac{\pi}{m}} T(\theta) e^{-jnm\theta} d\theta \tag{9}$$

Inserting this description of the reticle transmittance function (Eqns. (7), (8) and (9)) in the flux expression (Eqn. (6)), and reversing the order of summation and integration, we can write

$$F(t) = I(t)\left[\mathring{A}_0 + \sum_{n=1}^{\infty} \mathring{A}_n(t) \right] \tag{10}$$

where

$$\mathring{A}_0 = 2D \int_{\alpha - \arcsin\left(\frac{\delta}{D}\right)}^{\alpha + \arcsin\left(\frac{\delta}{D}\right)} \frac{c_0}{2} \cos(\alpha - \theta) \sqrt{D^2 \cos^2(\alpha - \theta) - (D^2 - \delta^2)}\, d\theta \tag{11}$$

and

$$\mathring{A}_n(t) = 2D \int_{\alpha - \arcsin\left(\frac{\delta}{D}\right)}^{\alpha + \arcsin\left(\frac{\delta}{D}\right)} c_n \cos(nm\theta + \phi_n) \cos(\alpha - \theta) \sqrt{D^2 \cos^2(\alpha - \theta) - (D^2 - \delta^2)}\, d\theta \tag{12}$$

Evaluating $\mathring{A}_0$ (Eqn. (11)), we get

$$\mathring{A}_0 = Dc_0 \int_{\alpha - \arcsin\left(\frac{\delta}{D}\right)}^{\alpha + \arcsin\left(\frac{\delta}{D}\right)} \cos(\alpha - \theta) \sqrt{D^2 \cos^2(\alpha - \theta) - (D^2 - \delta^2)}\, d\theta \tag{13}$$

Let $\theta' = \alpha - \theta$. Then get

$$\mathring{A}_0 = Dc_0 \int_{\arcsin\left(\frac{\delta}{D}\right)}^{-\arcsin\left(\frac{\delta}{D}\right)} \cos(\theta') \sqrt{D^2 \cos^2\theta' - (D^2 - \delta^2)}\, d(-\theta') \tag{14}$$

Since the integrand is even,

$$\begin{aligned} \mathring{A}_0 &= 2D\delta c_0 \int_0^{\arcsin\left(\frac{\delta}{D}\right)} \cos(\theta') \sqrt{\left(\frac{D}{\delta}\right)^2 \cos^2\theta' - \left(\frac{D}{\delta}\right)^2 + 1}\, d\theta' \\ &= 2D\delta c_0 \int_0^{\arcsin\left(\frac{\delta}{D}\right)} \cos(\theta') \sqrt{1 - \left(\frac{D}{\delta}\right)^2 \sin^2\theta'}\, d\theta' \end{aligned} \tag{15}$$

From tables (Beyer,1987), Eqn. (15) becomes

$$\begin{aligned} \mathring{A}_0 &= 2D\delta c_0 \left[\frac{\sin\theta'}{2} \sqrt{1 - \left(\frac{D}{\delta}\right)^2 \sin^2\theta'} + \frac{1}{2}\frac{\delta}{D} \arcsin\left(\frac{D}{\delta}\sin\theta'\right) \right]_0^{\arcsin\left(\frac{\delta}{D}\right)} \\ &= \frac{c_0}{2}\pi\delta^2 \end{aligned} \tag{16}$$

Define

$$A_0 \triangleq \mathring{A}_0 = \frac{c_0}{2}\pi\delta^2 \tag{17}$$

Likewise, for $\mathring{A}_n$ (Eqn. (12)),

$$\mathring{A}_n(t) = 2Dc_n \int_{\alpha - \arcsin\left(\frac{\delta}{D}\right)}^{\alpha + \arcsin\left(\frac{\delta}{D}\right)} \cos(nm\theta + \phi_n)\cos(\alpha - \theta)\sqrt{D^2\cos^2(\alpha - \theta) - (D^2 - \delta^2)}\, d\theta \tag{18}$$

For simplification, change the integration variable to $\theta' = \alpha - \theta$. Also, expand the first cosine term in Eqn. (18) . Then

$$\begin{aligned} \mathring{A}_n(t) &= 2Dc_n \int_{\arcsin\left(\frac{\delta}{D}\right)}^{-\arcsin\left(\frac{\delta}{D}\right)} \cos(nm(\alpha - \theta') + \phi_n)\cos\theta'\delta\sqrt{(\tfrac{D}{\delta})^2\cos^2\theta' - ((\tfrac{D}{\delta})^2 + 1)}\, d(-\theta') \\ &= 2D\delta c_n \int_{-\arcsin\left(\frac{\delta}{D}\right)}^{\arcsin\left(\frac{\delta}{D}\right)} \Bigg[\cos(nm\alpha + \phi_n)\cos nm\theta'\cos\theta' \sqrt{1 - \left(\frac{D}{\delta}\right)^2 \sin^2\theta'} \\ &\quad + \sin(nm\alpha + \phi_n)\sin nm\theta'\cos\theta' \sqrt{1 - \left(\frac{D}{\delta}\right)^2 \sin^2\theta'} \Bigg] d\theta' \end{aligned} \tag{19}$$

The first term in the integrand of Eqn. (19) is an even function, while the second term is an odd function in θ' and the integral of an odd function taken symmetrically about the origin vanishes. Therefore,

$$\mathring{A}_n(t) = 2D\delta c_n \cos(nm\alpha + \phi_n)\int_0^{arcsin\left(\frac{\delta}{D}\right)} 2\cos\theta' \cos nm\theta' \sqrt{1 - \left(\frac{D}{\delta}\right)^2 \sin^2\theta'}\, d\theta' \qquad (20)$$

It can be shown (Gedance,1961,Eqn. 9 and 10)[5] that if $\frac{\delta}{D} \ll 1$ and $\frac{nm\delta}{D} < 1$, then

$$\frac{nm}{\pi}\int_0^{arcsin\left(\frac{\delta}{D}\right)} 2\cos\theta' \cos nm\theta' \sqrt{1 - \left(\frac{D}{\delta}\right)^2 \sin^2\theta'}\, d\theta' \approx J_1\left(\frac{nm\delta}{D}\right) \qquad (21)$$

where $J_1\left(\frac{nm\delta}{D}\right)$ is the first order Bessel function of the argument $\left(\frac{nm\delta}{D}\right)$.

Then

$$\mathring{A}_n(t) \approx \frac{2\pi}{nm} D\delta c_n \cos(nm\alpha + \phi_n) J_1\left(\frac{nm\delta}{D}\right) \qquad (22)$$

From the geometry of the situation (See Figure 1 on page 14.), the triangle formed by the centres of the reticle (O_{RET}), target and rotation of the target image about the reticle (O_{ROT}) gives

$$D^2 = R_T^2 + r^2 - 2R_T r \cos(\omega_r t - \theta_T) \qquad (23)$$

and

$$\alpha = arctan\left(\frac{r\sin\omega_r t - R_T \sin\theta_T}{r\cos\omega_r t - R_T\cos\theta_T}\right) \qquad (24)$$

Establishing ρ as a normalized offset distance, $\frac{R_T}{r}$, then

$$D = r\sqrt{1 - 2\rho\cos(\omega t - \theta_T) + \rho^2} \qquad (25)$$

and

$$\alpha = arctan\left(\frac{\sin\omega_r t - \rho\sin\theta_T}{\cos\omega_r t - \rho\cos\theta_T}\right) \qquad (26)$$

---

5 See Appendix A for a demonstration, by series expansion, of this approximation.

$\mathring{A}_n$ can then be written in the condensed form

$$\mathring{A}_n(t) \approx A_n \cos \Theta_n(t) \tag{27}$$

where

$$A_n \triangleq \frac{2\pi}{nm} r\sqrt{1 - 2\rho \cos(\omega t - \theta_T) + \rho^2}\, \delta c_n J_1\left(\frac{nm\delta}{r\sqrt{1 - 2\rho \cos(\omega t - \theta_T) + \rho^2}} \right) \tag{28}$$

and

$$\Theta_n(t) \triangleq nm \arctan\left(\frac{\sin \omega_r t - \rho \sin \theta_T}{\cos \omega_r t - \rho \cos \theta_T} \right) + \phi_n \tag{29}$$

Note that for $\rho \ll 1$, $A_n(t) \approx$ constant. Note also from Eqns. (27) and (29) that the information on the position (ρ , θ_T) is carried in the angle. i.e. the target image motion and reticle interaction gives rise to a frequency modulation (FM). If the reticle pattern is such that the conditions $\frac{\delta}{D} \ll 1$ and $\frac{nm\delta}{D} < 1$ can be met[6] , then

$$F(t) \approx I(t)\left(A_0 + \sum_{n=1}^{N} A_n(t) \cos \Theta_n(t) \right) \tag{30}$$

where N is large but not violating the condition.

D. INSTANTANEOUS FREQUENCY

We now develop an expression for the instantaneous frequency of the flux signal as a step towards determining the information carried in the FM.

The flux signal, $F(t)$ is then bandpass filtered. Let's call the bandpass filtered signal $F_b(t)$. In general, a bandpass filtered signal can be represented in quadrature form or complex envelope form. i.e.,

$$F_b(t) \equiv P(t) \cos \omega_c t - Q(t) \sin \omega_c t \tag{31}$$

---

6 A seeker with a wagon wheel reticle would normally be designed to have the target image of approximately the same size as the width of the transparent spokes of the reticle, at the radius at which the target image rotates on the reticle. This would give the greatest target-to-background discrimination. Also, during a subsequent bandpass filtering operation (which will be describe later), the higher order components (associated with n in one of the conditions) of the reticle-generated signal are removed. Thus, in practice, in the vicinity of the design point of the reticle seeker, the two conditions of $\frac{\delta}{D} \ll 1$ and $\frac{nm\delta}{D} < 1$ can usually be met.

or

$$F_b(t) \equiv Re\left\{g(t)e^{j\omega_c t}\right\} \tag{32}$$

where, in this instance, if m is the number of cycles of transmittance changes that a point on the image goes through in one rotation about the reticle, then $\omega_c = m\omega_r$. The two forms given in Eqns. (31) and (32) are related by

$$g(t) = P(t) + jQ(t) \tag{33}$$

From the quadrature components $P(t)$ and $Q(t)$, we get the instantaneous frequency of that signal[7] (Roberts,1977) as

$$\omega_i(t) = \omega_c + \frac{P(t)\dot{Q}(t) - Q(t)\dot{P}(t)}{P^2(t) + Q^2(t)} \tag{34}$$

In a step reminiscent of synchronous or coherent demodulation of an FM signal, but using the scene rotation frequency as the reference frequency, we can extract the in-phase and quadrature-phase components of the signal. Later, we will show that this in fact gives the position of the target. To get an easily recognizable expression for the position in the end, we also include a scaling factor ($\frac{r}{\pi m}$) , at this stage. The in-phase component, $i(\tau)$, and quadrature phase component, $q(\tau)$, are described by

$$\begin{bmatrix} i(\tau) \\ q(\tau) \end{bmatrix} = \frac{r}{\pi m} \int_{\frac{\theta_T(\tau)-\pi}{\omega_r}}^{\frac{\theta_T(\tau)+\pi}{\omega_r}} \omega_i(t) \begin{bmatrix} \cos \omega_r t \\ \sin \omega_r t \end{bmatrix} dt \tag{35}$$

Note that we can only find the position vector a half-cycle behind current time because the integration takes place over a full cycle.

E. SIMPLIFIED RETICLE AND JAMMING SIGNAL

It is rather tedious to continue the analysis generally. So that we do not lose sight of the forest for the trees, we shall consider a special case of a reticle and of a jamming signal.

---

7 Essentially the instantaneous frequency is given by the differentiation of the phase of $F_b(t)$, with respect to time, and offset by the carrier frequency.

We can simplify the reticle transmission function to a single sinusoidal azimuthal variation, reducing the Fourier summation description of the reticle to a single term, besides the constant term. i.e.,

$$T(\theta) = \frac{1}{2} + \frac{1}{2}\cos[m(\theta - \phi_r)] \tag{36}$$

In terms of the quantities defined in Eqn. (8),

$c_0 = 1$

$c_1 = \frac{1}{2}$

$\phi_1 = -m\phi_r$

$c_n = 0$ for $n > 1$

Then, from Eqns. (17), (28) and (29), we get

$$A_0 = \frac{\pi\delta^2}{2}, \tag{37}$$

$$A_1(t) = \frac{2\pi}{m}\,\delta r\sqrt{1 - 2\rho\cos(\omega t - \theta_T) + \rho^2}\; J_1\left(\frac{m\delta}{r\sqrt{1 - 2\rho\cos(\omega t - \theta_T) + \rho^2}}\right) \tag{38}$$

and

$$\Theta_1(t) = m\left[\arctan\left(\frac{\sin\omega_r t - \rho\sin\theta_T}{\cos\omega_r t - \rho\cos\theta_T}\right) - \phi_r\right] \tag{39}$$

We now have a description of the component of the signal that results from the interaction of the target and the reticle, in the seeker.

F. VARIABLE IRRADIANCE FROM JAMMING

To investigate the potential for jamming, we apply an optical signal combining a constant target irradiance with a sinusoidal jamming signal. The irradiance , $I(t)$, is then described by

$$I(t) = I_{tgt} + I_j[1 + \cos\Theta_j(t)] \tag{40}$$

where I_{tgt} is the target irradiance

and $I_j[1 + \cos\Theta_j(t)]$ is the jammer irradiance which oscillates between 0 and $2I_j$.

Rearranging Eqn. (40) , we get

$$I(t) = I_c + I_j \cos \Theta_j(t) \tag{41}$$

where

$$I_c = I_{tgt} + I_j \tag{42}$$

is the unvarying component of the irradiance.
The flux signal for this special case is

$$F(t) = [I_c + I_j \cos \Theta_j(t)][A_0 + A_1(t) \cos \Theta_1(t)] \tag{43}$$

After high-pass filtering, the D.C. term, $I_c A_0$, will be rejected by the filter, and we get the bandpass signal

$$F_b(t) = \sum_{k=1}^{4} F_k \cos \phi_k(t) \tag{44}$$

where

$F_1 \triangleq I_c A_1(t)$ $\quad \phi_1 \triangleq \Theta_1(t)$
$F_2 \triangleq I_j A_0$ $\quad \phi_2 \triangleq \Theta_j(t)$
$F_3 \triangleq I_j A_1(t)$ $\quad \phi_3 \triangleq \Theta_j(t) - \Theta_1(t)$
$F_4 \triangleq I_j A_1(t)$ $\quad \phi_4 \triangleq \Theta_j(t) + \Theta_1(t)$

In complex envelope form,

$$F_b(t) = Re\{g(t)e^{j\omega_c t}\} \tag{45}$$

where

$$g(t) = \sum_{n=1}^{4} F_k e^{j(\phi_k(t) - \omega_c t)} \tag{46}$$

For compactness in subsequent expressions, let

$$\Phi_k(t) \triangleq \phi_k(t) - \omega_c t \quad . \tag{47}$$

To find the instantaneous frequency of the bandpass signal, we need first to find the quadrature components ($P(t)$ and $Q(t)$) of the bandpass signal. This is done using Eqns. (31) and (32) with Eqns. (46) and (47). We then get

$$\begin{aligned} P(t) &= Re\{g(t)\} \\ &= \sum_{n=1}^{4} F_k \cos \Phi_k(t) \end{aligned} \tag{48}$$

and

$$\begin{aligned} Q(t) &= Im\{g(t)\} \\ &= \sum_{n=1}^{4} F_k \sin \Phi_k(t) \end{aligned} \tag{49}$$

Also,

$$P^2(t) + Q^2(t) = \sum_{k=1}^{4} \sum_{l=1}^{4} F_k F_l \cos(\Phi_k(t) - \Phi_l(t)) \tag{50}$$

Taking the derivatives of the quadrature components described by Eqns. (48) and (49) , we get

$$\dot{P}(t) = - \sum_{n=1}^{4} \dot{\Phi}_k(t) F_k \sin \Phi_k(t) \tag{51}$$

and

$$\dot{Q}(t) = \sum_{n=1}^{4} \dot{\Phi}_k(t) F_k \cos \Phi_k(t) \tag{52}$$

Also, combining Eqns. (48), (49), (51), (52), gives

$$P(t)\dot{Q}(t) - Q(t)\dot{P}(t) = \sum_{k=1}^{4} \sum_{l=1}^{4} \dot{\Phi}_k(t) F_k F_l \cos(\Phi_k(t) - \Phi_l(t)) \tag{53}$$

Substituting Eqns. (53) and (50) in Eqn. (34) , the instantaneous frequency in this case is described by

$$\omega_i(t) = \omega_c + \frac{\sum_{k=1}^{4}\sum_{l=1}^{4} \dot{\Phi}_k(t) F_k F_l \cos(\Phi_k(t) - \Phi_l(t))}{\sum_{k=1}^{4}\sum_{l=1}^{4} F_k F_l \cos(\Phi_k(t) - \Phi_l(t))} \tag{54}$$

Now we define a jam-to-signal-plus-jam ratio, β_j, and further restrict the analysis to the case of small target offset from centre. Let $\beta_j \triangleq \frac{I_j}{I_c} = \frac{I_j}{I_{tgt} + I_j}$. If $\rho \ll 1$ (i.e., small target offset from centre), then

$$A_0 \approx A_1(t) \approx A_c \tag{55}$$

Hence

$$\frac{I_j A_c}{I_c A_c} \approx \frac{F_2}{F_1} \approx \frac{F_3}{F_1} \approx \frac{F_4}{F_1} \approx \beta_j \quad , \tag{56}$$

and we then get

$$\omega_i(t) = \omega_c + \frac{\sum_{k=1}^{4}\sum_{l=1}^{4} \dot{\Phi}_k(t) \beta_k \beta_l \cos(\Phi_k(t) - \Phi_l(t))}{\sum_{k=1}^{4}\sum_{l=1}^{4} \beta_k \beta_l \cos(\Phi_k(t) - \Phi_l(t))} \tag{57}$$

where

$$\beta_k = \begin{cases} 1 & if \quad k = 1 \\ \beta_j & if \quad k \neq 1 \end{cases} \tag{58}$$

and

$$\beta_l = \begin{cases} 1 & if \quad l = 1 \\ \beta_j & if \quad l \neq 1 \end{cases} \tag{59}$$

G. SPECIAL CASES

Let us now examine this result in the two limits of $\beta_j = 0$, no jamming, and $\beta_j = 1$, the infinite jamming case.

1. No-jamming case

Consider the no-jamming case when $I_j = 0$. i.e., when $\beta_j = 0$. Then

$$\beta_k = \begin{cases} 1 & \text{if } k = 1 \\ 0 & \text{if } k \neq 1 \end{cases} \tag{60}$$

and

$$\beta_l = \begin{cases} 1 & \text{if } l = 1 \\ 0 & \text{if } l \neq 1 \end{cases} \tag{61}$$

Substituting Eqns. (60) and (61) in Eqn. (57), we get

$$\begin{aligned} \omega_i(t) &= \omega_c + \frac{\dot{\Phi}_1(t)(1)^2}{(1)^2} \\ &= \omega_c + \dot{\phi}_1(t) - \omega_c \\ &= \dot{\phi}_1(t) \\ &= m\omega_r \left(\frac{1 - \rho \cos(\omega_r t - \theta_T)}{1 - 2\rho \cos(\omega_r t - \theta_T) + \rho^2} \right) \end{aligned} \tag{62}$$

Now that we have the instantaneous frequency of the signal, we will show that the coherent demodulation of Eqn. (35) does indeed give the position of the target. For the in-phase component,

$$\begin{aligned} i &= \frac{1}{\pi m} \int_{\frac{\theta_T - \pi}{\omega_r}}^{\frac{\theta_T + \pi}{\omega_r}} \omega_i(t) r \cos \omega_r t dt \\ &= \frac{1}{\pi m} \int_{\frac{\theta_T - \pi}{\omega_r}}^{\frac{\theta_T + \pi}{\omega_r}} m\omega_r \left(\frac{1 - \rho \cos(\omega_r t - \theta_T)}{1 - 2\rho \cos(\omega_r t - \theta_T) + \rho^2} \right) r \cos \omega_r t dt \end{aligned} \tag{63}$$

Defining the change of variable $\theta' = \omega_r t - \theta_t$ and expanding the trigonometric terms, we convert the integral into the form,

$$i = \frac{r}{\pi}\int_{-\pi}^{\pi} \frac{\cos\theta'\cos\theta_T - \sin\theta'\sin\theta_T - \rho\cos\theta_T\cos^2\theta' + \rho\sin\theta_T\sin\theta'\cos\theta'}{1 - 2\rho\cos(\omega_r t - \theta_T) + \rho^2}\, d\theta'$$
$$= \frac{2r\cos\theta_T}{\pi}\int_{0}^{\pi} \frac{\cos\theta' - (\rho/2)\cos 2\theta' + (\rho/2)}{1 - 2\rho\cos(\omega_r t - \theta_T) + \rho^2}\, d\theta' \tag{64}$$

From the tables of integrals (Gradshteyn 1980) we can evaluate this definite integral, as

$$\begin{aligned} i &= \frac{2r\cos\theta_T}{\pi}\left[\frac{\pi\rho}{2}\right] \\ &= r\rho\cos\theta_T \\ &= R_T\cos\theta_T \end{aligned} \tag{65}$$

which is in fact the x component of the target position. Similarly, from the quadrature-phase component, we get

$$q = R_T\sin\theta_T \tag{66}$$

which is the y component of the target position.

Hence the target location in two dimensions is now determined. (Note that whether or not there is jamming, the missile seeker, not knowing any better, will still perform the same procedure, described above, to try to extract the target position.)

2. Infinitely powerful jammer

Let us now consider the case in which we have an infinitely powerful jammer, i.e. $\beta_j = 1$ This case gives an instantaneous frequency expression that is not simple. To gain further insight, we will restrict the bandpass filter to an even narrower band about the carrier frequency (ω_c) of the flux-derived signal. The upper limit of the bandpass is just above twice the carrier frequency. Mathematically, we make Φ_3 and Φ_4 zero. Then Eqn. (57) becomes

$$\begin{aligned} \omega_i(t) &= \omega_c + \frac{\dot\Phi_1(t) + \dot\Phi_2(t) + \left[\dot\Phi_1(t) + \dot\Phi_2(t)\right]\cos\left[\Phi_1(t) - \Phi_2(t)\right]}{2 + 2\cos\left[\Phi_1(t) - \Phi_2(t)\right]} \\ &= \frac{1}{2}\left[\dot\Theta_1(t) + \dot\Theta_j(t)\right] \end{aligned} \tag{67}$$

And if the jamming waveform is similar in form to the reticle modulation waveform (as given in Eqn. (39)), and the jammer's equivalent of the reticle rotation frequency is $\omega_{rj} = \omega_r$, then the position coordinates of the apparent target location are :

$$\begin{bmatrix} \frac{1}{2}(R_T \cos\theta_T + R_j \cos\theta_j) \\ \frac{1}{2}(R_T \sin\theta_T + R_j \sin\theta_j) \end{bmatrix} \tag{68}$$

where R_j & θ_j are the jamming parameters corresponding to R_T & θ_T of the reticle. Note the effective pointing direction of the seeker to the apparent target is that for the centroid of the combination of the target signal and the jamming signal.

H. SOME OBSERVATIONS ON THE ANALYSIS RESULTS

The jamming signal cannot dominate the target signal because the jamming signal is itself modulated by the relative motion of the jamming spot and the reticle.

The analysis here is of a reticle that has a transmissivity function that varies gradually in a sinusoidal manner in the azimuth direction. For manufacturing ease, most of these reticles in real missiles will have more sharply changing transmissivities. However, to limit noise, the signal from the detector will eventually have to be bandlimited. Thus this analysis is a good first order approximation for the real missile.

It should be noted from the analysis that the conscan reticle seeker does not derive its information from the amplitude envelope. This being the case, AGC jamming techniques may not prove to be particularly effective against the conscan reticle seeker.

I. SIMULATION

Numerical analysis was performed to examine the intermediate cases of β_j . For simplicity and computation speed, only the narrow band version of the analysis was incorporated in this simulation program. i.e.,

$$\omega_i(t) = \omega_c + \frac{\sum_{k=1}^{2}\sum_{l=1}^{2} \dot{\Phi}_k(t)\beta_k\beta_l \cos(\Phi_k(t) - \Phi_l(t))}{\sum_{k=1}^{2}\sum_{l=1}^{2} \beta_k\beta_l \cos(\Phi_k(t) - \Phi_l(t))} \tag{69}$$

$$= m\omega_r + \frac{\dot{\Phi}_1(t) + \beta_j^2\dot{\Phi}_2(t) + [\dot{\Phi}_1(t) + \dot{\Phi}_2(t)]\beta_j \cos[\Phi_1(t) - \Phi_2(t)]}{1 + \beta_j^2 + 2\beta_j \cos[\Phi_1(t) - \Phi_2(t)]}$$

Eqn. (69) was then inserted into Eqn. (63) and the corresponding equation for the y-axis, and was transformed into computer code. At the same time, to incorporate the missile aerodynamics, the 2D position vector computation from the seeker was inserted into a version of the TACTICS IV program (Meisberger,1983) which was ported to a microcomputer. TACTICS IV is a time step simulation of a missile flight. It computes the relative positions and velocities of a target and a missile, takes the seeker-derived position (with noise added, if desired), applies a proportional navigation guidance law, and integrates the effects of a commanded acceleration to obtain the new position and velocity of the missile. The modified TACTICS IV, which we call TACTICS IV (IR) incorporates the infrared seeker behaviour with an infrared jammer. The seeker routine was patched so that it will branch to the new infrared seeker routine when desired.[8] The parameters required for the seeker are essentially the parameters of Eqn. (69). In addition, the tabulated output file of the missile and target flight profiles was modified slightly to be more easily read by a graphics program.[9] The listing of the infrared seeker portion of that program can be found in Appendix B.

An example of the result of an air-to-air missile flight simulation is in Figure 2 on page 29 . In this example, the missile is launched at the target from a position directly behind the target. The target does not evade, but continues in a straight and level flight path. Figure 3 on page 30 is the input data to the TACTICS IV (IR) program, for this example. In this particular case, the missile departs from the target in a spiral-like path. Note the increase in miss distance to 700 feet with the infrared jammer on, as compared to the 3 feet case when there is no jammer.[10]

This study should be continued with sensitivity analysis studies and optimizations to identify the optimal jamming parameters.

---

8 This is done by making the ISEEK parameter of the input data table equal to 5.

9 The postprocesser described by Meisberger (1983) was not ported to the microcomputer. Instead, a commercial package, STATGRAPHICS, was used for the graphical output.

10 The no-jammer case was simulated in a separate run, with β_j effectively zero.

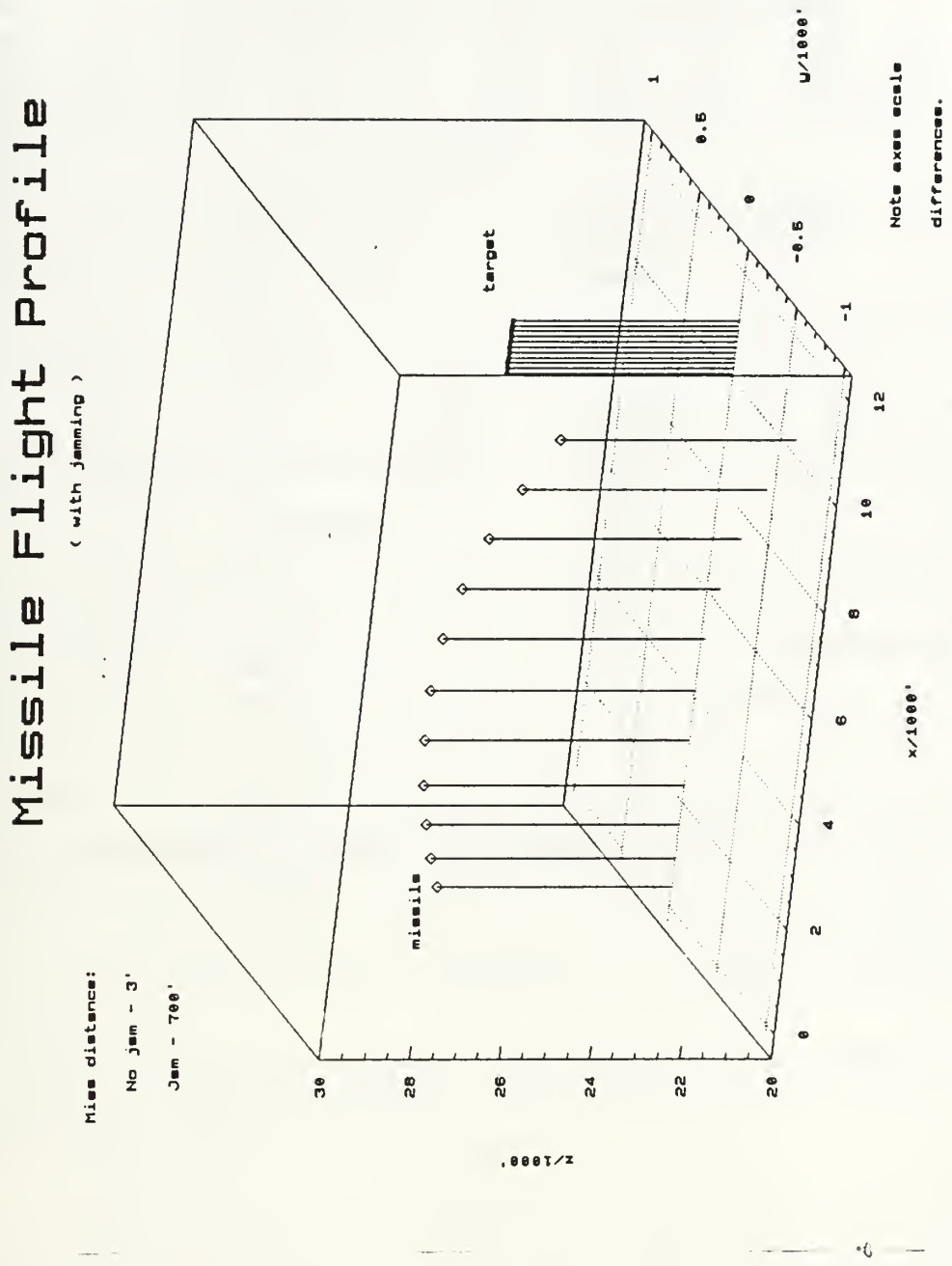

Figure 2. Missile flight profile (with jamming): Missile and target flying from left to right.

```
1
    0.20    0.80    1.50     2.0     2.35    2.87    3.95    4.60       0       0
   0.235   0.240    1.05   0.910   0.830   0.745   0.630   0.580       0       0
    1.04    1.04    1.04    0.93    0.86    0.90    0.90    0.87       0       0
   0.116   0.127   0.198   0.162   0.141   0.113   0.070   0.051       0       0
     0.0     4.0     6.0     8.0    10.0    12.0    14.0    30.0    50.0       0
     4.0     4.0     4.0     4.0     4.0     4.0     4.0     4.0     4.0       0
TEST     STT
0 001          0.0          0.0       25000.0          0.9          0.0
0 006         28.6      10000.0          0.0      25000.0         0.20
0 011          0.0          0.0          1.0         6.00         0.00
0 016        191.0     -10.00000    -0.000000          0.0          0.0
0 021          0.1          0.0          0.0          0.1          0.0
0 026         0.01         0.01          0.0         0.70         30.0
0 031          0.0          0.0     0.136000          0.0         -1.5
0 036          1.0      15000.0        0.001          0.0         11.0
0 041          0.0         0.50         0.05         30.0          0.0
0 046          6.0          0.0          0.0          0.0      20000.0
0 051       6788.0          0.0          5.0  0.0000000005        100.0
0 056         0.90         15.0       2300.0         0.00         21.8
0 061          4.3          0.0          3.0        359.0         0.55
0 066          1.2          8.0          2.4         0.02        160.0
0 071       2000.0          0.0          1.0         0.05          0.1
0 076          0.0          0.0          0.0          0.0          0.0
- 0
```

Figure 3. TACTICS IV (IR) Input data for missile flight (with jamming)

VI. RECOMMENDED COUNTERMEASURES

In summary, given the scenario considered here, the most promising short term countermeasure solution is the infrared jammer. The infrared jammer has a good chance of working if it has the following characteristics:-

- For all aspect coverage, the infrared energy sources should radiate all around the aircraft. This would imply more than one source element, as there is no single point on the aircraft that has equal visibility in all directions.
- The power output of the jammer source, in the band that the missile detector is using, needs to be at least equal to the target signature in that band and in the same direction.
- The jammer should be able to modulate its infrared power emitted such that the waveform is similar to what the seeker forms when it views a steadily radiating target.

The analysis done here is only a paper study, using what are intended to be (hopefully) typical parameter values. The actual signatures of these aircraft under various conditions must be measured to provide accurate input. The infrared jammer source and modulation scheme must actually be verified by test and evaluation with real hardware to determine if the assumptions and analysis are correct. e.g.,can we find IR sources that can provide enough in-band energy on the seeker's detector. We have not determined yet the optimal modulation scheme against the conscan (FM) seeker. Neither have we considered the optimal modulation scheme when there are more than one type of missile. Evaluation must be extended to these cases to ensure that modulation schemes, while effective against a particular type of missile seeker, do not decrease the miss-distance for other seeker types.

This study must also be extended to the third generation scanning spot seeker threat, which is increasing with time.

VII. CONCLUSION

Low speed / low manoeuvrability aircraft are currently quite susceptible to being killed in attacks by the ubiquitous infrared missiles. A theoretical analysis applied to an encounter simulation seems to indicate that it is possible to use the infrared jammer to defeat second generation infrared missiles. The theoretical analysis of a simplified case of a conical scan reticle with frequency modulation jamming leads to expressions for the target's position, as seen by the missile seeker, under no-jamming and under infinitely-powerful-jamming conditions. The intermediate-power case is dealt with by numerical analysis for a selected, non-optimal situation, as the closed form solution is not immediately apparent. The analysis indicates successful jamming in the situation studied. In the scenario where the infrared missile is an almost continuous threat during the aircraft's flight, infrared jammers and low visual signature paints, and perhaps low infrared signature paints, are short-term solutions that are potentially useful in increasing the survivability of these aircraft by reducing their susceptibility to infrared missile kills.

APPENDIX A. VALIDATION OF THE APPROXIMATION

We want to demonstrate that if $\frac{\delta}{D} \ll 1$ and $\frac{nm\delta}{D} < 1$, then

$$\frac{nm}{\pi}\int_0^{\arcsin\left(\frac{\delta}{D}\right)} 2\cos\theta'\cos nm\theta'\sqrt{1-\left(\frac{D}{\delta}\right)^2\sin^2\theta'}\,d\theta' \approx J_1\left(\frac{nm\delta}{D}\right) \tag{70}$$

For convenience, let

$$x \triangleq \left(\frac{nm\delta}{D}\right) \tag{71}$$

and call the left hand side of Eqn. (70), $f_{\cos}(x)$. Now the first order Bessel function in series form is

$$J_1(x) = \frac{x}{2}\sum_{k=0}^{\infty}\frac{(-1)^k x^{2k}}{2^{2k}k!(k+1)!} \tag{72}$$

Expanding the first few terms of this series, we get

$$J_1(x) \approx \frac{1}{2}x - \frac{1}{16}x^3 + \frac{1}{384}x^5 - \ldots \tag{73}$$

Expanding the integrand in the left hand side of Eqn. (70), using the Taylor series, and integrating, we get

$$\begin{aligned} f_{\cos}(x) \approx\ & \frac{1343}{80\pi}x - \frac{181}{840\pi}x^3 + \frac{3}{280\pi}x^5 - \ldots \\ & - \frac{1}{8\pi}\left(\frac{\delta}{D}\right)^2 x + \frac{17}{420\pi}\left(\frac{\delta}{D}\right)^2 x^3 + \frac{1}{168\pi}\left(\frac{\delta}{D}\right)^2 x^5 + \ldots \end{aligned} \tag{74}$$

If $\left(\frac{\delta}{D}\right) \ll 1$, the terms in the second row of Eqn. (74) are small in relation to those in the first row and hence can be neglected. Computing the coefficients of x,

$$f_{\cos}(x) \approx \frac{1}{1.97}x - \frac{1}{14.6}x^3 + \frac{1}{293}x^5 - \ldots \tag{75}$$

Comparing Eqn. (73) and Eqn. (75), if $\frac{nm\delta}{D} < 1$, then

$$f_{\cos}(x) \approx J_1(x) \tag{76}$$

which is what we set out to show.

APPENDIX B. TACTICS IV (IR) PARTIAL LISTING

```
{**************************************
   Program listing of the infrared seeker
   portion of TACTICS IV (IR).
   Requires TurboPascal 5.0 and the
   TurboPascal Numerical Toolbox.
 **************************************}
unit tac8s;

interface
uses tac8g;

  {$I floatdef.inc}
procedure csj_seeker(time : float;
                     var seeker_theta_prev,
                     seeker_phi_prev,
                     seeker_theta_cur,
                     seeker_phi_cur : float);

procedure GetOutputFile_Name(var OutFile : text;
                             var FileName : string;
                             default_filename : string);

procedure get_root_name_of_files(var FileName : string;
                                 default_filename : string);

implementation


  {$I-}                          { Disable I/O error trapping }
  {$R+}                          { Enable range checking }

uses
  Integrat, Dos, Crt, Common, Funct;

const
  m = 12;
  m_j = 12;
  r = 1.0;
  w_r_rev = 40;
  del_w_r_rev_default = 0.39;
  phic_r = 0.0;
  phic_j = 0.78540;
  rho_init = 0.0;
  rho_j_default = 0.499;
  thetac_T_init = 0.0;
  thetac_j_default = 0.0;
  del_theta_default = 3.14159265/3;
  beta_j_default = 1.0/2.0;
  filt_cons = 1.0;
  max_move_step = 0.1;
  filename_csj_default = 'CSJ.OUT';
  focal_length = 57.0;

var
  w_r, w_r_j, del_w_c, del_w_r, beta_j : float
  x_tj, y_tj, range_tgt, theta_tgt : float;
  x_tl, y_tl, range_tgtl, theta_tgtl : float;
var t_cyc, t_cyc_j : float;
  ref_t, del_t_2 : float;
  u_llm, l_llm : float;
  del_theta : float;
  rho_j, rho_j_start : float;
  del_w_r_rev : float;
  i : integer;
  consl : text;
  rho, rho_step : float;
  thetac_T, thetac_j : float;
  temp_beta : float;
  new_x, new_y : float;
  del_range, del_x, del_y : float;
  FileName : string;

var
  LowerLimit, UpperLimit : float; { Limits of integration }
  Tolerance : float;              { Tolerance in the answer }
  MaxIntervals : integer;         { Maximum number of subintervals used }
  { to approximate the integral }
  Integral : float;               { Value of the integral }
  NumIntervals : integer;         { Number of subintervals used }
  { to approximate integral }
  Error : byte;                   { Flags if something went wrong }


  {$F+}

  function beta(t : float) : float;
  var tt : float;
  begin
    beta := beta_j;
  end;                            {function beta}


  function theta_o(t : float) : float;
  var numer, denom : float;
  begin
    numer := sin(w_r*t)-(rho*sin(thetac_T));
    denom := cos(w_r*t)-(rho*cos(thetac_T));
    theta_o := m*(arctan(numer/denom)-phic_r);
  end;

  function theta_j(t : float) : float;
  begin
```

```
  theta_j := m_j*(arctan((sin((w_r+del_w_r)*t)-(rho_j*sin(thetac_j)))/
                         (cos((w_r+del_w_r)*t)-(rho_j*cos(thetac_j))))-phic_j);
end;

function thetadot_o(t : float) : float;
begin
  thetadot_o := m*w_r*((1-rho*cos(w_r*t-thetac_T))/
                       (1-2*rho*cos(w_r*t-thetac_T)+rho*rho));
end;

function thetadot_j(t : float) : float;
var numer, denom : float;
begin
  numer := (1-rho_j*cos((w_r+del_w_r)*t-thetac_j));
  denom := (1-2*rho_j*cos((w_r*t+del_w_r)-thetac_j)+rho_j*rho_j);
  thetadot_j := m_j*(w_r+del_w_r)*(numer/denom);
end;


function phi_j(t : float) : float;
var tj : float;
begin
  tj := theta_j(t);
  phi_j := tj-(m*w_r*t);
end;

function phidot_j(t : float) : float;
var tdj : float;
begin
  tdj := thetadot_j(t);
  phidot_j := tdj-(m*w_r);
end;

function phi_o(t : float) : float;
var tho : float;
begin
  tho := theta_o(t);
  phi_o := tho-(m*w_r*t);
end;

function phidot_o(t : float) : float;
var tdo : float;
begin
  tdo := thetadot_o(t);
  phidot_o := tdo-(m*w_r);
end;

function w_1(t : float) : float;
var betat, oo, pj, pdo, pdj, numer, denom : float;
begin
  betat := beta(t);
  oo := phi_o(t);
  pj := phi_j(t);
  pdo := phidot_o(t);
  pdj := phidot_j(t);
  numer := betat*betat*pdj+odo+(pdj+odo)*betat*cos(pj-po);
  denom := 1+2*betat*cos(oj-po)+betat*betat;
  w_1 := m*w_r+(numer/denom);
end;

{$F-}

{$F+}
function TNTargetF(t : float) : float;

  {--------------------------------------------------}
  {-         This is the function to integrate      -}
  {--------------------------------------------------}

var temp1 : float;

begin
  temp1 := w_1(t);
  TNTargetF := temp1*r*cos(w_r*t);
end;                                { function TNTargetF }
{$F-}


{$F+}
function TNTargetF_sin(t : float) : float;

  {--------------------------------------------------}
  {-         This is the function to integrate      -}
  {--------------------------------------------------}

var temp1 : float;

begin
  temp1 := w_1(t);
  TNTargetF_sin := temp1*r*sin(w_r*t);
end;                                { function TNTargetF_sin }
{$F-}




procedure Initialize(var LowerLimit : float;
                     var UpperLimit : float;
                     var Integral : float;
                     var Tolerance : float;
                     var MaxIntervals : integer;
                     var NumIntervals : integer;
                     var Error : byte);

  {-------------------------------------------------------------------}
  {- Output: LowerLimit, UpperLimit, Integral, Tolerance,            -}
  {-         MaxIntervals, NumIntervals, Error                       -}
  {-                                                                 -}
  {- This procedure initializes the above variables to zero          -}
  {-------------------------------------------------------------------}

begin
```

```
  writeln;
  LowerLimit := 0;
  UpperLimit := 0;
  Integral := 0;
  Tolerance := 0;
  MaxIntervals := 0;
  NumIntervals := 0;
  Error := 0;
end;                              { procedure Initialize }


procedure Re_Initialize(
  var Integral : float;
  var NumIntervals : integer;
  var Error : byte);

begin
  Integral := 0;
  NumIntervals := 0;
  Error := 0;
end;                              { procedure Re_Initialize }

procedure get_root_name_of_files(var FileName : string;
                                  default_filename : string);
begin
  writeln;
  FileName := default_filename;
  write('Enter root of file name [', FileName, '] ');
  readln(FileName);
  if FileName = '' then FileName := default_filename;
end;                              { procedure GetOutputFile_Name }


procedure GetOutputFile_Name(var OutFile : text;
                             var FileName : string;
                             default_filename : string);
var
  Ch : char;

begin
  repeat
    Ch := 'Y';
    writeln;
    FileName := default_filename;
    write('Enter file name [', FileName, '] ');
    readln(FileName);
    if FileName = '' then FileName := default_filename;
    assign(OutFile, FileName);
    reset(OutFile);
    if ioresult = 0 then          { The file already exists. }
      begin
        close(OutFile);
        writeln;
        write('This file already exists. ');
        write('Write over it (Y/N)? ');
        Ch := upcase(ReadKey);
        writeln(Ch);
        if Ch = 'Y' then assign(OutFile, FileName);
      end;
    if Ch = 'Y' then
      begin
        rewrite(OutFile);
        IOCheck;
      end;
  until ((Ch = 'Y') and not(IOerr));
end;                              { procedure GetOutputFile_Name }

procedure GetData(var LowerLimit : float;
                  var UpperLimit : float;
                  var Tolerance : float;
                  var MaxIntervals : integer);

  {-------------------------------------------------------------}
  {- Output: LowerLimit, UpperLimit, Tolerance, MaxIntervals  -}
  {-                                                          -}
  {- This procedure assigns values to the above variables     -}
  {- from keyboard input                                      -}
  {-------------------------------------------------------------}

  procedure GetLimits(var LowerLimit : float;
                      var UpperLimit : float);

    {-----------------------------------------------------------}
    {- Output: LowerLimit, UpperLimit                          -}
    {-                                                         -}
    {- This procedure assigns values to the limits of          -}
    {- integration from keyboard input                         -}
    {-----------------------------------------------------------}

  begin
    repeat
      repeat
        LowerLimit := 0.0;
        IOCheck;
      until not IOerr;
      writeln;
      repeat
        UpperLimit := 2*pi/w_r;
        IOCheck;
      until not IOerr;
      if LowerLimit = UpperLimit then
        begin
          writeln;
          writeln('       The limits of integration must be different.');
          writeln;
        end;
    until LowerLimit <> UpperLimit;
  end;                            { procedure GetLimits }

  procedure GetTolerance(var Tolerance : float);

    {-------------------------------------------------}
    {- Output: Tolerance                             -}
```

```
    {-                                                  -}
    {- This procedure reads in the accepted Tolerance -}
    {- from the keyboard.                              -}
    {-------------------------------------------------}
  const default_tolerance = 1e-2;
  begin
    writeln;
    repeat
      Tolerance := default_tolerance;
      write('Tolerance in answer: (> 0): ');
      ReadFloat(Tolerance);
      IOCheck;
      if Tolerance <= 0 then
        begin
          IOerr := true;
          Tolerance := default_tolerance;
        end;
    until not IOerr;
  end;                              { procedure GetTolerance }

  procedure GetMaxIntervals(var MaxIntervals : integer);

    {-------------------------------------------------}
    {- Output: MaxIntervals                           -}
    {-                                                -}
    {- This procedure reads in the maximum number of  -}
    {- subintervals to be used in approximating the   -}
    {- integral.  Input is from the keyboard.         -}
    {-------------------------------------------------}

  begin
    writeln;
    repeat
      MaxIntervals := 1000;
      write('Maximum number of subintervals (> 0): ');
      ReadInt(MaxIntervals);
      IOCheck;
      if MaxIntervals <= 0 then
        begin
          IOerr := true;
          MaxIntervals := 1000;
        end;
    until not IOerr;
  end;                              { procedure GetMaxIntervals }

begin                               { procedure GetData }
  GetLimits(LowerLimit, UpperLimit);
  GetTolerance(Tolerance);
  GetMaxIntervals(MaxIntervals);
  {  GetOutputFile(OutFile); }
end;                                { procedure GetData }

procedure Results(LowerLimit : float;
                  UpperLimit : float;
                  Tolerance : float;
                  MaxIntervals : integer;
                  Integral : float;
                  NumIntervals : integer;
                  Error : byte);

  {-------------------------------------------------------------}
  {- This procedure outputs the results to the device OutFile -}
  {-------------------------------------------------------------}

begin
  writeln(OutFile);
  writeln(OutFile, 'Lower Limit:':35, LowerLimit:25);
  writeln(OutFile, 'Upper Limit:':35, UpperLimit:25);
  writeln(OutFile, 'Tolerance:':35, Tolerance:25);
  writeln(OutFile, 'Maximum number of subintervals:':35, MaxIntervals:5);
  writeln(OutFile, 'Number of subintervals used:':35, NumIntervals:5);
  if Error = 3 then
    DisplayWarning;
  if Error in [1, 2] then
    DisplayError;

  case Error of
    0 : writeln(OutFile, 'Integral:':25, Integral);

    1 : writeln(OutFile, 'The tolerance must be greater than zero.');

    2 : writeln(OutFile,
                'The maximum number of intervals must be greater than zero.');

    3 : begin
          writeln(OutFile, 'The integral was not found with ', NumIntervals,
                  ' subintervals.');
          writeln(OutFile, 'The integral thus far: ', Integral);
        end;
  end;                              { case }
end;                                { procedure Results }

procedure get_beta_j(var beta_j : float);
begin
  writeln;
  repeat
    beta_j := beta_j_default;
    write('beta_j : ');
    ReadFloat(beta_j);
    IOCheck;
    if beta_j < 0 then
      begin
        IOerr := true;
        beta_j := beta_j_default;
      end;
  until not IOerr;
end;                                { procedure get_beta_j }

procedure get_del_theta(var del_theta : float);
begin
  writeln;
  repeat
    del_theta := del_theta_default;
```

```
    write('del_theta : ');
    ReadFloat(del_theta);
    IOCheck;
    if del_theta < 0 then
      begin
        IOerr := true;
        del_theta := del_theta_default;
      end;
  until not IOerr;
end;                                { procedure get_del_theta }

procedure get_rho_j(var rho_j : float);
begin
  writeln;
  repeat
    rho_j := rho_j_default;
    write('rho_j : ');
    ReadFloat(rho_j);
    IOCheck;
    if rho_j < 0 then
      begin
        IOerr := true;
        rho_j := rho_j_default;
      end;
  until not IOerr;
  rho_j_start := rho_j;
end;                                { procedure get_del_theta }

procedure get_thetac_j(var thetac_j : float);
begin
  writeln;
  repeat
    thetac_j := thetac_j_default;
    write('thetac_j : ');
    ReadFloat(thetac_j);
    IOCheck;
    if thetac_j < 0 then
      begin
        IOerr := true;
        thetac_j := thetac_j_default;
      end;
  until not IOerr;
end;                                { procedure get_del_theta }

procedure get_del_w_r_rev(var del_w_r_rev : float);
begin
  writeln;
  repeat
    del_w_r_rev := del_w_r_rev_default;
    write('del_w_r_rev : ');
    ReadFloat(del_w_r_rev);
    IOCheck;
    if del_w_r_rev < 0 then
      begin
        IOerr := true;
        del_w_r_rev := del_w_r_rev_default;
      end;
  until not IOerr;
end;                                { procedure get_del_theta }


procedure init_params;
begin
  get_beta_j(beta_j);
  get_del_theta(del_theta);
  get_rho_j(rho_j);
  get_thetac_j(thetac_j);
  get_del_w_r_rev(del_w_r_rev);

  w_r := w_r_rev*2*pi;
  del_w_r := del_w_r_rev*2*pi;

  t_cyc := 2*pi/w_r;
  w_r_j := (w_r+del_w_r);
  t_cyc_j := 2*pi/w_r_j;
  ref_t := thetac_j/w_r_j;
  del_t_2 := del_theta/2/w_r_j;
  u_lim := ref_t+del_t_2;
  while u_lim < t_cyc_j do u_lim := u_lim-t_cyc_j;
  l_lim := ref_t-del_t_2;
  while l_lim < 0 do l_lim := l_lim+t_cyc_j;

  rho := rho_init;
  thetac_T := thetac_T_init;

end;


procedure write_one_iteration_line(var out_file : text);
begin
  writeln(out_file,
          i:4,
          ' ', rho_j:6:3,
          ' ', rho:7:3,
          ' ', thetac_T:7:3,
          '>', x_tj:7:3,
          ' ', y_tj:7:3,
          ' ', range_tgt:7:3,
          ' ', theta_tgt:7:3,
          ' ', new_x:7:3,
          ' ', new_y:7:3);
end;



procedure csj_seeker(time : float;
                     var seeker_theta_prev,
                     seeker_phi_prev,
                     seeker_theta_cur,
                     seeker_phi_cur : float);
var xp, yp, xc, yc, xd, yd : float;
```

```
  begin
    UpperLimit := time;
    LowerLimit := UpperLimit-t_cyc;
    xp := seeker_theta_prev*focal_length;
    yp := seeker_phi_prev*focal_length;
    xc := seeker_theta_cur*focal_length;
    yc := seeker_phi_cur*focal_length;
    xd := xp-xc;
    yd := yp-yc;
    rho := sqrt((xd*xd)+(yd*yd));
    thetac_T := atan2(yd, xd);

    Adaptive_Gauss_Quadrature(LowerLimit, UpperLimit, Tolerance, MaxIntervals,
                              Integral, NumIntervals, Error, @TNTargetF);
    x_tj := Integral/(pi*m);
    Re_Initialize(Integral, NumIntervals, Error);
    Adaptive_Gauss_Quadrature(LowerLimit, UpperLimit, Tolerance, MaxIntervals,
                              Integral, NumIntervals, Error, @TNTargetF_sin);
    y_tj := Integral/(pi*m);

{  range_tgt:=sqrt(x_tj*x_tj+y_tj*y_tj);
  theta_tgt:=atan2(y_tj,x_tj);
  del_range:=range_tgt;
  del_x:=del_range*cos(theta_tgt);
  del_y:=del_range*sin(theta_tgt);}

    del_x := x_tj;
    del_y := y_tj;

    xc := xp-del_x;
    yc := yp-del_y;
    seeker_theta_cur := xc/focal_length;
    seeker_phi_cur := yc/focal_length;
    seeker_theta_prev := seeker_theta_cur;
    seeker_phi_prev := seeker_phi_cur;
  end;

  procedure write_table_header(var out_file : text);
  begin
    writeln(out_file);
    writeln(out_file,
            '   i',
            '  rho_j',
            '    rho',
            '   tht_T',
            '    x_tj',
            '    y_tj',
            '  rng_tg',
            '  tht_tg',
            '   new_x',
            '   new_y');
  end;

  procedure write_end_iterations_line(var out_file : text);
  begin
    writeln(out_file,
            i:4,
            ' ', rho_j:6:3,
            ' ', rho:7:3,
            ' ', thetac_T:7:3,
            '> End...');
  end;

  procedure write_file_header;
  begin
    writeln(csj_file);
    writeln(csj_file, 'm    = ', m:4);
    writeln(csj_file, 'm_j = ', m_j:4);
    writeln(csj_file, 'r    = ', r:7:3);
    writeln(csj_file, 'beta_j          = ', beta_j:7:3);
    writeln(csj_file, 'w_r_rev         = ', w_r_rev:4);
    writeln(csj_file, 'del_w_r_rev     = ', del_w_r_rev:7:3);
    writeln(csj_file, 'phic_r          = ', phic_r:7:3);
    writeln(csj_file, 'phic_j          = ', phic_j:7:3);
    writeln(csj_file, 'rho_init        = ', rho_init:7:3);
    writeln(csj_file, 'rho_j_start     = ', rho_j_start:7:3);
    writeln(csj_file, 'del_theta       = ', del_theta:7:5);
    writeln(csj_file, 'thetac_T_init = ', thetac_T_init:7:3);
    writeln(csj_file, 'theta_j         = ', theta_j:7:5);
    writeln(csj_file, 'filt_cons       = ', filt_cons:7:5);
    writeln(csj_file, 'focal_length    = ', focal_length:7:3);
    writeln(csj_file);
    writeln(csj_file);
    write_table_header(csj_file);
    writeln(csj_file);
  end;

begin                                   { main program }
  ClrScr;
  get_root_name_of_files(default_filename, init_default_filename);
  GetOutputFile_Name(csj_file, FileName, default_filename+'csj');
  init_params;
  InitIalize(LowerLimit, UpperLimit, Integral, Tolerance, MaxIntervals,
             NumIntervals, Error);
  GetData(LowerLimit, UpperLimit, Tolerance, MaxIntervals);

  range_tgt := 0;
  theta_tgt := 0;
  rho := rho_init;
  thetac_T := thetac_T_init;
  write_file_header;

end.                                    { unit csjunit}
```

LIST OF REFERENCES

ASD,Wright-Patterson AFB, ASD XR-TR-75-1-VOL-1, (AD-B009 668L) *ASDIR-II, Vol. 1, User Manual*, Stone, C.W. and Tate, S.E., Dec 1975.

Ball, Robert E., *The Fundamentals of Aircraft Combat Survivability Analysis and Design*, AIAA, 1985.

Beyer, William H., *CRC Standard Mathematical Tables*, 28th Edition, p.274, Eqn. 439, CRC Press, Inc., 1987.

Cooper, A.W., *Electro-Optics Devices and Principles*, Class notes for the PH3208 Course, Fall 1988.

Couch, Leon W. II, *Digital and Analog Communication Systems*, 2nd Edition, Macmillan, 1987.

Gedance, Alan R., "Comparison of Infrared Tracking Systems", *Applied Optics*, Vol. 51, No.10, pp. 1127-1130, Oct 1961.

General Electric Co., Aircraft Engine Group, *Preliminary Infrared Radiation Emissions Predictions (PIREP)*, Vol. I, Nov 1976.

Gradshteyn I.S. & Ryzhik, I.M., *Table of Integrals, Series and Products*, p. 366, Eqn. 3.613.2, Academic Press, 1980.

General Dynamics, *The World's Missile Systems*, General Dynamics, Aug 1988.

Higby, R.F., Brown, R.C. & Goodell, J.B., *Evaluation of Infrared Countermeasures*, Interim Technical Report (Model Methodology), Prepared for U.S. Army Aviation Command by Westinghouse Electric Corp., 26 Jun 1972.

Loral Electro-Optical Systems, *Electro-Optical Warfare Presentation for the Naval Postgraduate School*, 8 Dec 1988.

Loral Electro-Optical Systems, P89-02-583, *Challenger Proposal and Installation Information*, p. 3-10, Table 3.2, 10 Feb 1989.

Meisberger, Joseph J., *Implementation of the Missile Target Engagement Simulation Program, TACTICS IV, and Associated Postprocessor Program for use at the Naval Postgraduate School*, Master's Thesis, Naval Postgraduate School, Monterey, California, Dec 1983.

Nicholas, Ted, & Rossi, Rita, *U.S. Missile Data Book 1989*, 13th Edition, Data Search Associates, Oct 1988.

Roberts, J.H., *Angle Modulation: The Theory of System Assessment*, p. 19, Peter Peregrinus, 1977.

Schaffer, Van A., *Susceptibility Assessment for the Conceptual and Preliminary Design of Aircraft*, Master's Thesis, Naval Postgraduate School, Monterey, California, Jun 1982.

Suzuki, Keizoh,"Analysis of Rising-Sun Reticle" *Optical Engineering* , Vol. 18, No.3, pp. 350-351, May-Jun 1979.

BIBLIOGRAPHY

Biberman, Lucien M., *Reticles in Electro-Optical Devices*, Pergamon Press, 1966.

Hudson Richard D., *Infrared System Engineering*, John Wiley & Sons, Inc., 1969.

Marshall, William E., *Implementation of the Bank-to-Turn Missile Profile in TACTICS IV*, Master's Thesis, Naval Postgraduate School, Monterey, California, Dec 1984.

Wolfe, William L. & Zissis, George J. ed., *The Infrared Handbook*, Revised edition, The Infrared Information and Analysis (IRIA) Center, Environmental Research Institute of Michigan, 1985.

INITIAL DISTRIBUTION LIST

		No. Copies
1.	Defense Technical Information Center Cameron Station Alexandria, VA 22304-6145	2
2.	Library, Code 0142 Naval Postgraduate School Monterey, CA 93943-5002	2
3.	Dir. Research Admin., Code 012 Naval Postgraduate School Monterey, CA 93943	1
4.	Electronic Warfare Academic Group (Attn. Prof. J. Sternberg, Code 73Sn) Naval Postgraduate School Monterey, CA 93943	1
5.	Prof. A. W. Cooper, Code 61Cr Naval Postgraduate School Monterey, CA 93943	2
6.	Prof. R. E. Ball, Code 67Bp Naval Postgraduate School Monterey, CA 93943	2
7.	Maj. Chia, Hock Teck HQ RSAF MINDEF Building Gombak Drive Off Upper Bukit Timah Road Republic of Singapore (2366)	3
8.	Office of the Chief of Naval Operations Pentagon (OP-762) Washington, D.C. 20350-2000	1
9.	Commander Naval Air Systems Command (Attn. Mr. Dale B. Atkinson, AIR-5164) Washington, D.C. 20361-5160	1